Metabolism of (*R*)- and (*S*)-3-(Phenylamino)propane-1,2-diol in C57BL/6- and A/J-Strain Mice. Identification of New Metabolites with Potential Toxicological Significance to the Toxic Oil Syndrome

Jordi Bujons,[†] Margarita G. Ladona,*[,‡] Angel Messeguer,[†] Anna Morató,[†] and Coral Ampurdanés[‡]

Department of Biological Organic Chemistry, Instituto de Investigaciones Químicas y Ambientales de Barcelona, and Department of Medical Bioanalysis, Instituto de Investigaciones Biomédicas de Barcelona, Consejo Superior de Investigaciones Científicas, Barcelona, Spain

Received January 5, 2001

The Toxic Oil Syndrome was a massive food-borne intoxication that occurred in Spain in 1981. Epidemiological studies point to 3-(phenylamino)propane-1,2-diol (PAP) derivatives as the putative toxic agents. We report further identification of metabolites cleared in urine of A/J and C57BL/6 mice in which (*R*)- and (*S*)-3-(phenylamino)propane-1,2-diol were administered intraperitoneally. This investigation is an extension of previous studies carried out with the racemic compound [Ladona, M. G., Bujons, J., Messeguer, A., Ampurdanés, C., Morató, A., and Corbella, J. (1999) *Chem. Res. Toxicol.* **12**, 1127−1137]. Both PAP enantiomers were extensively metabolized, and several metabolites were eliminated in urine. The HPLC profiles of the urine samples of both mouse strains treated with each enantiomer were qualitatively similar, but differences were found in a relatively higher proportion of several detected metabolites in mice treated with (*R*)-PAP compared with those treated with (*S*)-PAP. The main urine metabolite continues to be 2-hydroxy-3-(phenylamino)propanoic acid (**1**), which confirms our previous results obtained with *rac*-PAP. In addition to the detection of other metabolites already reported in our previous paper, interesting evidence is provided on the presence of 4-aminophenol and paracetamol conjugates in the urine samples from both mouse strains. The detection of these metabolites suggests the in vivo formation of quinoneimine PAP derivatives. Indeed, some quinoneimine species (**11** and **12**), as well as other PAP metabolites (**13**) that bear modifications in the alkyl chain, have been tentatively identified in mouse urine. These metabolic findings might imply a potential toxicological significance for the Toxic Oil Syndrome.

Introduction

The Toxic Oil Syndrome (TOS)[1] appeared in Spain in 1981 as a massive food-borne intoxication that affected more than 20 000 people (*1*). TOS was attributed to the ingestion of rapeseed oil, which had been adulterated with aniline, illegally refined, and delivered for human consumption (*1*−*6*). Two types of chemical species derived from aniline were identified in oil batches, i.e., fatty acid anilides (amides) and fatty acid esters of 3-(phenylamino)propane-1,2-diol (PAP) (aromatic amines) (*1, 7, 8*), with the latter, the PAP esters, being strongly associated with TOS (*8, 9*). In particular, epidemiological studies has revealed that the levels of the 1,2-dioleyl ester of 3-(phenylamino)propane-1,2-diol (OOPAP) correlate with patient morbidity in the corresponding households; therefore, this compound is currently considered to be the putative toxic compound responsible for the intoxication (*9, 10*). OOPAP was generated by chemical processes during oil refining at the ITH Co., and the epidemic was considered to have emerged from a single source in that refinery (*11*).

Extensive efforts to investigate the potential toxicity of aniline derivatives in animal species were carried out with unsuccessful results to reproduce the full spectrum of symptoms observed in humans (*12*). However, few studies reported partial toxicity in mice; e.g., PAP and its mono-oleyl ester (OPAP) were toxic to some mouse strains when administered intraperitoneally (*13, 14*), but lacked toxicity when administered orally. In this respect, it has also been shown that, when administered orally to rats, OOPAP is hydrolyzed in the intestine to the corresponding mono-oleyl ester and PAP (*15*). Although

* To whom correspondence should be addressed at Cartagena 401, AT-2, 08024 Barcelona, Spain. E-mail: mglqob@cid.csic.es.

[†] Department of Biological Organic Chemistry, Instituto de Investigaciones Químicas y Ambientales de Barcelona.

[‡] Department of Medical Bioanalysis, Instituto de Investigaciones Biomédicas de Barcelona.

[1] Abbreviations: TOS, Toxic Oil Syndrome; EMS, Eosinophilia-Myalgia Syndrome; OLA, oleanilide; PAP, 3-(phenylamino)propane-1,2-diol; OPAP, monooleyl ester of PAP.; OOPAP dioleyl ester of PAP.; MPAP, DPAP, mono and diacyl derivatives of PAP.; PAA, 3-(phenylamino)-L-alanine; *β*-NF, *β*-naphthoflavone; TEAA, triethylammonium acetate; TEAC, triethylammonium hydrogen carbonate; PBS, phosphate buffered saline (137 mM NaCl, 2.7 mM KCl, 10 mM Na_2HPO_4, 1.8 mM KH_2PO_4, pH 7.4); BSTFA, *O,N*-bis(trimethylsilyl)trifluoroacetamide; EI-MS, electron impact mass spectrometry; HRP, horseradish peroxidase.

10.1021/tx010001k CCC: $20.00
Published on Web 07/31/2001

Chart 1. PAP and Related Structures Investigated as Putative Metabolites of PAP in C57BL/6- and A/J-Strain Mice

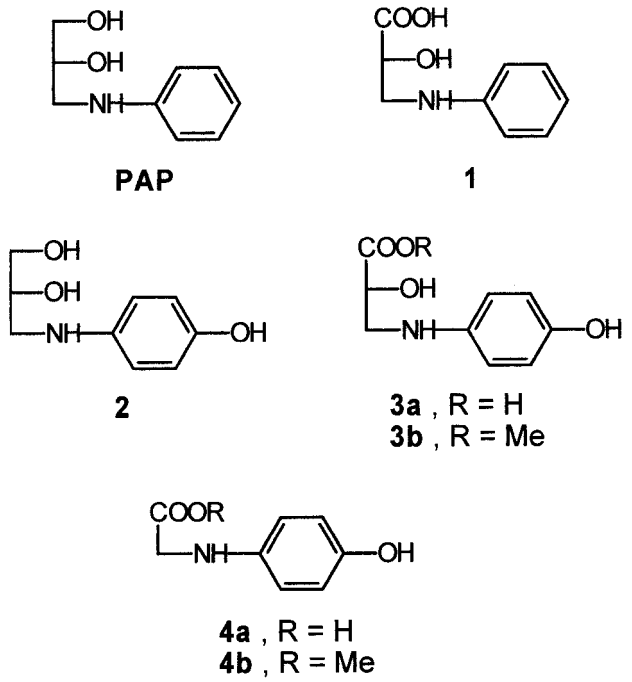

TOS disease was considered species-specific for humans (*12*), from animal studies it can be postulated that aniline derivative toxicokinetics may differ between animals and humans. Thus, to ascertain the potential toxicity of these compounds and seek an animal model, investigation efforts should focus on determining factors such as metabolism, distribution, and elimination in comparison between animals and humans.

Therefore, our research line focused on investigating the metabolic profile of TOS patients in parallel with determining PAP derivative metabolism and distribution in mouse strains, and, further, applying the acquired knowledge to obtain an animal model for in-depth analysis of TOS pathogenic mechanisms. In this respect, we recently reported that TOS survivors exhibit a specific metabolic profile determined by molecular analyses on genetic polymorphisms of enzyme metabolism (*16*). In addition, we have studied the biotransformation and clearance of racemic PAP (*rac*-PAP) in the C57BL/6 and A/J mouse strains (*17*), a well-known murine model for human acetylation polymorphism. Metabolic species of PAP (Chart 1) administered intraperitoneally, in particular 2-hydroxy-3-(phenylamino)propanoic acid **1**, were identified for the first time as major metabolites in the urine of these mouse strains. Nevertheless, the structure of additional minor PAP metabolites present in those urine samples remained to be elucidated. Further on this line of research, we investigated the in vitro stereoselectivity of the lipase-catalyzed hydrolysis of the mono and dioleyl PAP esters as a model of the transformations that PAP esters may undergo in the human intestinal tract.[2] The results of these studies indicate that these esters can be regio- and stereoselectively hydrolyzed and, therefore, that absorption through the intestinal cells into the human body of enantiomerically enriched PAP, MPAP, and DPAP can be expected. Consequently, enantiomeric distribution and metabolism differences should be taken into account in the toxicokinetics of these compounds and their association with TOS symptoms.

With these findings and the evidence of intestinal formation of PAP enantiomers, herein we extend our previous work on in vivo disposition in mice of *rac*-PAP by reporting the results of analogous studies carried out with the pure (*R*)- and (*S*)-PAP enantiomers. This study led us to the identification of new PAP metabolites in mouse urine samples which may have toxicological significance for TOS.

Materials and Methods

Chemicals and Reagents. Aniline (Aldrich, 99%) and glycidol (Merck, 98%) were previously distilled and stored at −20 °C. (*R*)- and (*S*)-glycidol, 4-aminophenol, *N*-(4-hydroxyphenyl)glycine, 4-acetamidophenol (paracetamol), and *O*,*N*-bis(trimethylsilyl)trifluoroacetamide (BSTFA) were obtained from Aldrich (Germany). [U-^{14}C]Aniline hydrochloride (129 mCi/mmol) was from Amersham (U.K.). Olive oil, β-glucuronidase from *Helix pomatia* and *Escherichia coli*, and β-naphthoflavone (β-NF) were obtained from Sigma (St. Louis, MO). Methanol, acetonitrile, isopropyl alcohol, dichloromethane, and other common solvents were of HPLC quality and were purchased from Merck (Darmstadt, Germany). Triethylammonium acetate (TEAA, 1 M, pH 7.0) and triethylammonium hydrogen carbonate (TEAC, 1 M, pH 8.4) buffers were obtained from Fluka (Switzerland). General laboratory reagents were obtained from local sources and were of analytical grade. OptiPhase 'HiSafe' cocktail was purchased from Fisons Chemicals (England).

Caution: *As PAP derivatives have been implicated in TOS, special precautions should be taken when handling these substances to avoid potential risks (use gloves, masks, and ventilated hood cabinets when handling solutions and powder).*

Synthesis of PAP Derivatives. Unless stated otherwise, organic solutions obtained from the treatment of crude reaction mixtures were dried over $MgSO_4$. Purification of metabolites by flash chromatography was performed using 35−70 μm silica gel (SDS, France). Reactions were monitored either by GC, HPLC, or TLC. GC analyses were performed on a Hewlett-Packard 5890 Series II gas chromatograph, provided with a FID detector and a 15 m HP-5 capillary column. HPLC analyses were performed on a Hewlett-Packard 1100 system provided with a DAD detector and a HP ODS Hypersil column (5 μm, 125 × 4 mm), using mixtures of HPLC grade acetonitrile and 10 mM TEAA (pH 6.8) buffer as eluents. Thin-layer chromatography (TLC) analyses were performed on Merck Kielsegel 60 F_{254} plates (aluminum sheets, 0.2 mm thickness) using mixtures of hexanes−EtOAc as eluents, and were developed by UV irradiation at 254 nm. Radioactivity was determined with an LKB 1217 Rackbeta scintillation counter following the addition of 10 mL of OptiPhase 'HiSafe' cocktail. The ^{1}H (300 MHz) and ^{13}C (75 MHz) NMR spectra were registered with a Varian Unity 300 spectrometer. Spectra were taken in neutralized $CDCl_3$ unless otherwise stated. Chemical shifts are given in ppm relative to tetramethylsilane for ^{1}H and deuteriochloroform for ^{13}C as internal standards. The GC/MS analyses and EI-MS spectra (70 eV) were obtained using a Fisons model MD 800 mass spectrometer coupled to a Fisons GC 8000 apparatus equipped with a 25 m HP-5 capillary column. Elemental microanalyses were carried out at the "Servei de Microanàlisi" of the I.I.Q.A.B. using a 1108 Carlo Erba analyzer.

[U-^{14}C]-*rac*-PAP (5.7 mCi/mmol) was prepared from [U-^{14}C]-aniline hydrochloride as previously described (*17*). (*R*)-PAP and (*S*)-PAP were synthesized by reaction of aniline with (*S*)- and (*R*)-glycidol, respectively, according to our previous experience.[2]

[2] Ladona, M. G., Morató, A., Messeguer, A., Ampurdanés, C., and Bujons, J. Stereoselective hydrolysis of 1,2-dioleyl-3-phenylaminopropane-1,2-diol by human pancreatic lipase and bovine lipoprotein lipase: toxicokinetic implications in Toxic Oil Syndrome. Manuscript in preparation.

Scheme 1. Synthetic Pathway for the Obtention of Quinoneimine 10

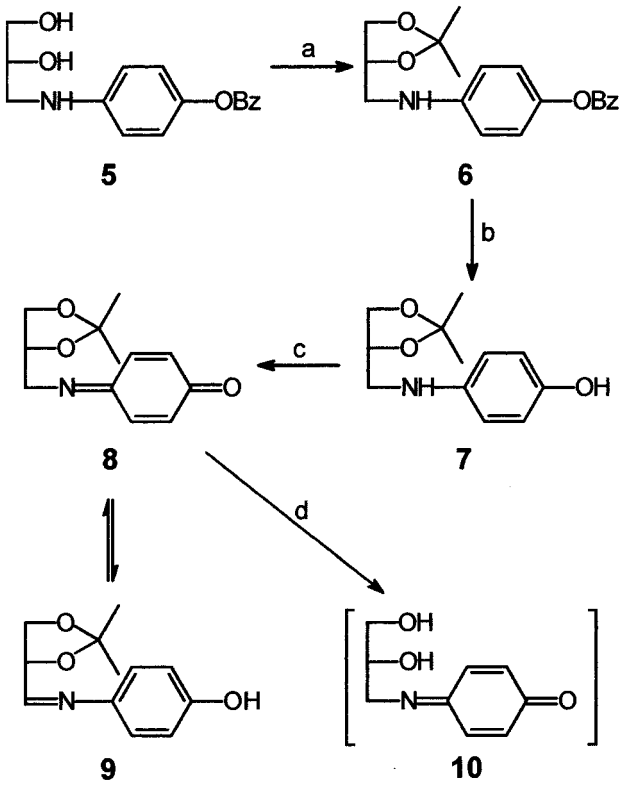

a) Acetone dimethylacetal, Amberlyst-15®, 80 °C, 73 %; b) H_2, Pd/C, EtOH, 85 %; c) Ag_2O, $CHCl_3$; d) HCl/MeOH

4-(4′-Benzyloxyphenyl)aminomethyl-2,2-dimethyl-1,3-dioxacyclopentane (6). This dioxolane was prepared from benzyloxy derivative **5** (Scheme 1) (*17*). Briefly, a mixture of **5** (0.24 g, 0.9 mmol), 2,2-dimethoxypropane (5 mL), and a catalytic amount of Amberlyst 15 was stirred for 2 h at 80 °C (GC monitoring). The crude reaction mixture was cooled, filtered, and evaporated. The residue was redissolved in *tert*-butyl methyl ether, washed with $NaHCO_3$, and dried. Final purification by column chromatography on silica gel (4:1 hexane/EtOAc) afforded 0.20 g (73% yield) of compound **6** as a yellow oil. ^{1}H NMR δ 7.35 (5 H″), 6.84 (d, 2 H, J = 9.0, H-3′, H-5′), 6.53 (d, 2 H, J = 9.0, H-2′, H-6′), 4.97 (2 H, CH_2Ph), 4.32 (m, 1 H, H−CO), 4.06 (dd, 1 H, J_1 = 8.2, J_2 = 6.4, CHH−O), 3.74 (dd, 1 H, J_1 = 8.2, J_2 = 6.4, CHH−O), 3.23 (dd, 1 H, J_1 = 12.4, J_2 = 4.4, CHH−N), 3.12 (dd, 1 H, J_1 = 12.4, J_2 = 6.6, CHH−N), 1.44 (s, 3 H, CH_3), 1.36 (s, 3 H, CH_3); ^{13}C NMR δ 151.5 (C-4′), 142.4 (C-1′),137.5 (C-1″), 128.4 (C-3″, C-5″), 127.7 (C-4″), 127.4 (C-2″, C-6″), 116.1 (C-3′, C-5′), 114.2 (C-2′, C-6′), 109.3 (H_3CCCH_3), 74.5 (CHO), 70.7 (CH_2Ph), 67.2 (CH_2O), 47.5 (CH_2N), 26.8 (CH_3), 25.3 (CH_3); EI-MS m/z 313(M^+), 91 (base peak). Elemental analysis for $C_{19}H_{23}NO_3$: C, 72.82; H, 7.40; N, 4.47. Found: C, 72.83; H, 7.40; N, 4.37.

4-(4′-Hydroxyphenyl)aminomethyl-2,2-dimethyl-1,3-dioxacyclopentane (7). A mixture of dioxolane **6** (0.10 g, 0.32 mmol) and 10% Pd/C (0.030 g, 0.032 mmol) in EtOH (7 mL) was stirred under a hydrogen atmosphere at 20 °C. When the reaction was completed (2 h, TLC monitoring), the crude reaction mixture was filtered and evaporated to give the desired product **7** (0.06 g, 85% yield). This compound was used without further purification. ^{1}H NMR δ 6.72 (d, 2 H, J = 9.0, H-3′, H-5′), 6.67 (d, 2 H, J = 9.0, H-2′, H-6′), 4.65 (2 H, NH, OH), 4.36 (m, 1 H, H-CO), 4.07 (dd, 1 H, J_1 = 8.4, J_2 = 6.3, CHH−O), 3.74 (dd, 1 H, J_1 = 8.4, J_2 = 6.0, CHH−O), 3.25 (dd, 1 H, J_1 = 12.5, J_2 = 4.2, CHH−N), 3.14 (dd, 1 H, J_1 = 12.5, J_2 = 7.2, CHH−N), 1.44 (s, 3 H, CH_3), 1.35 (s, 3 H, CH_3); ^{13}C NMR δ 150.7 (C-4′), 138.9 (C-1′), 116.5 (C-3′, C-5′), 116.3 (C-2′, C-6′), 109.7 (H_3CCCH_3), 73.7 (CHO), 67.1 (CH_2O), 49.2 (CH_2N), 26.9 (CH_3), 25.3 (CH_3); EI-MS m/z 223(M^+), 208, 122 (base peak); EI-MS (TMS derivative) m/z 295 (M^+), 194 (base peak).

Oxidation of Dioxolane 7. The oxidation of dioxolane **7** was carried out following the procedure described by Dahlin and Nelson for the case of *N*-acetyl-*p*-benzoquinoneimine (*18*). Thus, **7** (10 mg, 45 μmol) and Ag_2O (7 mg, 30 μmol) were stirred in dry chloroform (5 mL) at 20 °C until no further evolution of the substrate was observed (4 h, HPLC monitoring). The crude reaction mixture was filtered and the filtrate evaporated to dryness to give a residue which revealed the presence of imine **9** as the major compound, **9**: ^{1}H NMR δ 7.86 (d, 1 H, J = 5.1, HC=N), 7.05 (d, 2 H, J = 9.0, H-3′, H-5′), 6.81 (d, 2 H, J = 9.0, H-2′, H-6′), 4.76 (m, 1 H, H−CO), 4.29 (dd, 1 H, J_1 = 8.6, J_2 = 6.6, CHH−O), 4.05 (dd, 1 H, J_1 = 8.6, J_2 = 6.3, CHH−O), 1.50 (s, 3 H, CH_3), 1.44 (s, 3 H, CH_3); ^{13}C NMR δ 161.2 (C-3), 115.8 (C-3′, C-5′), 122.2 (C-2′, C-6′), 142.9 (C-1′), 155.1 (C-4′), 110.5 (C(CH_3)$_2$), 77.3 (C-2), 67.4 (C-1), 26.5 (CH_3), 25.4 (CH_3); EI-MS m/z 221 (M^+), 208, 120 (base peak); EI-MS (TMS derivative) m/z 293 (M^+), 235, 192 (base peak).

To follow the evolution of the reaction by ^{1}H NMR, the reaction was repeated by placing in an NMR tube 18 mg (81 μmol) of dioxolane **7** dissolved in 0.7 mL of anhydrous $CDCl_3$ and adding 22 mg of Ag_2O (81 μmol). The initial formation of a product was observed which was transformed into imine **9** in the course of several hours. The spectroscopic data of this intermediate were compatible with quinoneimine **8**: ^{1}H NMR δ 7.32 (dd, 1 H, J_1 = 10.3, J_2 = 2.6),[3] 7.14 (dd, 1 H, J_1 = 10.3, J_2 = 2.6),[3] 6.58 (m, 1 H, J_1 = 10.3, J_2 = 1.2),[3] 6.57 (m, 1 H, J_1 = 10.3, J_2 = 1.2),[3] 4.56 (m, 1 H, H−CO), 4.20 (dd, 1 H, J_1 = 8.4, J_2 = 6.5, CHH−O), 4.00 (dd, 1 H, J_1 = 15.0, J_2 = 5.9, CHH−N), 3.91 (dd, 1 H, J_1 = 15.0, J_2 = 6.2, CHH−N), 3.87 (dd, 1 H, J_1 = 8.4, J_2 = 6.0, CHH−O), 1.43 (s, 3 H, CH_3), 1.40 (s, 3 H, CH_3); ^{13}C NMR δ 142.8 (C_{Ar}H), 133.0 (C_{Ar}H), 131.7 (C_{Ar}H), 125.2 (C_{Ar}H), 109.7 (C(CH_3)$_2$), 75.5 (C-2), 67.6 (C-1), 56.2 (C-3), 26.8 (CH_3), 25.3 (CH_3). An aliquot of the crude mixture containing this intermediate was filtered, treated with BSTFA, and analyzed by GC/MS. The main peak detected was that of the *O*-silylated derivative of imine **9**, described above. In addition, a peak consistent with the structure of quinoneimine **8** was detected [EI-MS m/z 221 (M^+), 163, 120 (base peak)], but only as a minor component probably due to the decomposition of the product.

Animals. A/J and C57BL/6 mice (9−10 weeks old, three animals of each strain) used in the experiments were obtained from Charles River (France) and Criffa (Spain), respectively. Animals were kept in metabolic cages (Techniplast, Italy) for 3 days of acclimatization and induced with β-NF prior to administration of PAP. Protocols for induction treatment with β-NF and PAP administration to the animals were identical to those previously described (*17*). Identification of phenolic species and PAP acid metabolites in our previous study prompted us to induce mice with β-NF, since we expected that the enzymes induced by the *Ah*-receptor enzyme battery would contribute to the formation of such metabolic species. In this respect, we observed that in C57BL/6 mice the urine clearance of metabolites increased to levels similar to those observed in A/J mice when pretreated with β-NF. Thus, in the present investigation we used the same conditions, i.e., to treat mice with β-NF 80 mg/kg in olive oil distributed in three intraperitoneal injections. A single total dose of (*R*)- or (*S*)-PAP (250 mg/kg, average animal weight in each group: 22−24 g) spiked with 4 μCi of [U-^{14}C]-*rac*-PAP was given intraperitoneally. Urine and feces were collected over a 24 h period and the animals euthanized. Organs (lung, liver, kidney, heart, muscle, and spleen) were collected in cold PBS (pH 7.4) and stored at −80 °C until analysis.

^{14}C Radioactivity Measurements in Organic Tissue and Body Fluids. Urine samples (20 μL) were mixed with 10 mL

[3] The chemical shifts and coupling constants for these absorptions were confirmed through simulation using a LAOCOON based program included in the software of the Varian Unity 300 instrument.

of OptiPhase 'HiSafe' scintillation cocktail and counted. The radioactivity remaining in feces and tissues was counted in a similar manner after total organ homogenization in PBS buffer (pH 7.4). An aliquot of tissue homogenate (0.5−1 mL) was counted, and total ^{14}C disintegrations per minute in organs were calculated. For equipment decontamination purposes, remaining radioactivity, if any, in the cage cone-collectors, which would indicate a radioactivity loss during the collecting period (urine and feces), was measured.

Analytical Determinations in Biological Fluids. (1) High-Performance Liquid Chromatography (HPLC). HPLC analyses were conducted on a Millenium Waters system equipped with a 717 Autosampler and a 996 Photodiode Array Detector, coupled on-line to a Berthold LB 507 radioactivity monitor system. UV spectra were collected with a resolution of 3.6 nm. C-18 Kromasil 100, 5 μm particle size, 250 × 4.6 mm columns (Teknokroma, Spain) were used with 10 mM TEAA, pH 6.8 (solvent A), and acetonitrile (solvent B) as mobile phases. Gradient elutions consisted of an initial isocratic step (0−5 min) at 0.9 mL/min 95% A, followed by a linear ramp to reach 1.1 mL/min 60% A (5−20 min), and a final isocratic elution at 1.1 mL/min 60% A (20−30 min), similar to as previously described (*17*).

Urine samples were used as reported (*17*). Briefly, 50 μL of the urine samples was mixed with methanol (1:9 v/v) and centrifuged. Supernatants were injected directly into the HPLC system. For the separation of polar metabolites from PAP, urine samples were buffered with 100 mM triethylammonium hydrogen carbonate (TEAC, pH 8.4) and extracted with a mixture of dichloromethane−isopropyl alcohol (9:1) containing 1% ammonia. The organic extracts were evaporated and redissolved in TEAA (10 mM, pH 6.8)−acetonitrile (80:20) prior to the HPLC analysis, while the aqueous phases were analyzed directly.

Chemical and enzymatic procedures were used for conjugate cleavage and metabolite derivatization. The chemical procedure consisted of treatment of the direct-urine sample or aqueous-extract samples with 1 mL of 1 M HCl in methanol (HCl/MeOH) for 15 min at 90 °C followed by evaporation of the solvents with a stream of nitrogen. Direct-urine hydrolysates were further extracted at pH 8.4 (TEAC) as described above. Samples treated in this manner were subjected to either HPLC or GC/MS analysis. Enzymatic hydrolysis consisted of sample treatment with 2000 enzyme units/mL of sample-incubate of β-glucuronidase from *E. coli* or *H. pomatia* (which also exhibits sulfatase activity) in the appropriate buffers for 16 h at 37 °C. Hydrolysates were further extracted at pH 8.4 (TEAC) and processed as described above.

(2) Gas Chromatography/Mass Spectrometry (GC/MS). Samples for GC/MS analysis were lyophilized, redissolved in acetonitrile, and treated with BSTFA, as described by Adachi et al. (*19*), prior to injection into the GC/MS system described above. Samples treated with HCl/MeOH were also redissolved in acetonitrile after evaporation of solvents and injected either directly or treated with BSTFA before injection into the GC/MS system.

Results

Synthesis of PAP Derivatives. Synthesis of quinoneimine **10** was initially attempted by oxidation of the corresponding aminophenol precursor **2** using chemical [oxidation with Fremy's salt (*20*, *21*)] and enzymatic methods [HRP-catalyzed oxidation (*22*)]. However, efforts carried out for isolating the desired product were unsuccessful. An explanation of this failure could be the potential instability and high polarity expected for **10** which would account for the erratic results observed in the HPLC monitoring of the reaction course.[4] These antecedents advised us to design a synthesis where both hydroxyl groups were protected until the last step, thus facilitating the manipulation and monitoring of the different intermediates. Accordingly, the synthetic pathway shown in Scheme 1 was attempted. Protection of aminodiol **5** as acetonide followed by hydrogenolysis afforded phenol **7**. Treatment of **7** with silver oxide in chloroform (*18*) and close control of the reaction by HPLC and NMR revealed the initial formation of a major product which presented only a UV maximum at 271 nm, consistent with the oxidation of the aromatic ring. The NMR data of this compound are consistent with those expected for quinoneimine **8**, in particular, the four multiplets centered at 7.32, 7.14, 6.58, and 6.57 ppm in the ^1H NMR spectrum[3] which were assigned, respectively, to the four nonequivalent protons of the quinoneimine moiety. This intermediate in deuteriochloroform was slowly transformed into a new product which was identified as imine **9**, the compound resulting from the prototropic rearrangement of quinoneimine **8**. Especially, the presence of a doublet at 7.86 ppm assigned to the imine HC═N proton, an AB system (7.05 and 6.81 ppm) for the aromatic protons, and a multiplet at 4.76 ppm attributed to the HC−O− proton were in agreement with the imine structure. Moreover, the GC/MS analysis of silylated aliquots of this crude reaction mixture permitted the detection of a main product with the molecular ion at *m*/*z* 293 and the base peak at *m*/*z* 192. These peaks appeared 2 units below the corresponding peaks observed for the *O*-silylated derivative of phenol **7**, and are consistent with the imine **9** structure. Unfortunately, the occurrence of quinoneimine **8** could not be definitively confirmed by GC/MS owing to the decomposition of the product during the derivatization with BSTFA and/or the chromatographic process. In this respect, we systematically detected the presence of the phenol precursor **7** on GC/MS analysis of samples containing quinoneimine **8** as the major component (^1H NMR monitoring). It is worth noting that for the quinoneimine derived from paracetamol (*18*, *26*), as well as other quinones (*27*), the detection of products derived from their reduction due to traces of residual water in the ion source of the mass spectrometer has been reported.

Further analysis of the evolution of the above sample by NMR showed a progressive decrease in the absorptions attributed to imine **9**, which was concomitant to the appearance of a new compound identified as 4-aminophenol, based on its chromatographic and spectroscopic data (not shown). In addition, a doublet centered at 9.73 ppm (J = 1.8 Hz) indicative of the formation of an aldehyde species was also observed. All these results can be explained by the transformations postulated in Scheme 2. Thus, oxidation of aminophenol **7** would lead to the generation of quinoneimine **8**. This unstable intermediate would rearrange to give imine **9**, a compound that was identified in the crude reaction mixture. Finally, hydrolysis of the imine would give rise to 4-aminophenol and the corresponding aldehyde species. A similar process had been proposed for the evolution of the quinoneimine derived from *N*-(4-hydroxyphenyl)glycine (*28*), and a more detailed study of this class of rearrangement for *N*-alkyl monoquinoneimines has also been reported (*29*).

As anticipated, when the acetal deprotection of an aliquot from the above crude reaction mixture, taken

[4] It is noteworthy that the literature describes mainly examples of *N*-acylated quinoneimines, in particular the acetyl derivative (*18*), or few cases of quinoneimines where this moiety is forming part of a more complex condensed ring structure (*23*, *24*). The isolation of such electrophilic species is difficult because of their instability (*25*).

Scheme 2. Proposed Pathway for the Formation of 4-Aminophenol from Phenolic PAP Derivatives

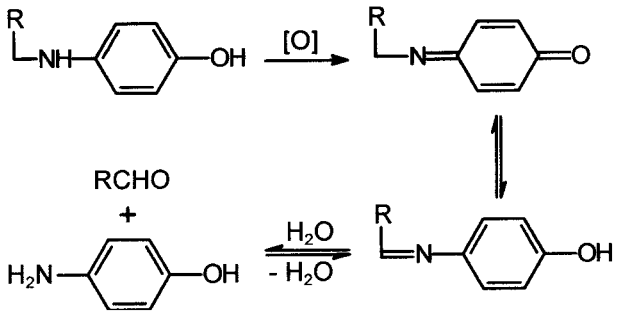

Table 1. ^{14}C-PAP Clearance in Urine and Feces in a 24 h Period

	(*S*)-PAP-treated mice[a]		(*R*)-PAP-treated mice[a]	
	A/J	C57BL/6	A/J	C57BL/6
^{14}C-PAP dose[b]	3.1×10^7	3.1×10^7	2.5×10^7	2.4×10^7
urine (mL)	2.00	2.00	1.23	1.80
% of dose	59	52	54	63
feces (g)	3.60	3.10	4.06	3.58
% of dose	0.45	0.54	1.80	0.80

[a] Three mice of each strain (total = 6) were placed together in a metabolic cage, constituting two groups treated either with (*R*)- or with (*S*)-PAP (250 mg/kg average animal weight). [b] [^{14}C]-*rac*-PAP total dose (dpm) administered together with the PAP enantiomer to each animal group. Urine and feces samples were collected over a 24 h period as detailed under Materials and Methods.

when the concentration of quinoneimine **8** was maximal, was assayed in mild acid media (HCl/MeOH), a complex HPLC profile was obtained from which the presence of quinoneimine **10** could not be inferred. Likewise, silylation of this crude reaction mixture yielded no peak by GC/MS with the mass spectrum expected for the silylated imine. However, the HPLC profile again revealed the presence of 4-aminophenol.

Attempts to generate quinoneimine **10** by direct oxidation of the phenolic PAP derivative **2** with Ag_2O in deuteriochloroform were also made (data not shown). Although it was possible to detect by ^{1}H NMR the initial formation of a product with a set of signals in the aromatic region similar to those described above for quinoneimine **8**, the more complex nature of this crude reaction mixture prevented us from carrying out further analysis.

^{14}C-Radioactivity Clearance. Table 1 depicts the radioactivity clearance observed in both mouse strains induced with β-NF after a single dose of each PAP enantiomer spiked with [^{14}C]-*rac*-PAP. As shown, we collected 52−60% of the radioactive dose in the urine samples over a 24 h period. In contrast, radioactivity clearance in fecal samples was in all cases less than 2%. This clearance profile was consistent with those previously reported for the racemate PAP (*17*). Similarly, the radioactivity content measured in the analyzed tissues was less than 1% of the total administered dose. Therefore, the differences in the urine radioactivity clearance observed between mice treated with each PAP enantiomer could be considered negligible, suggesting that both isomers are metabolized and eliminated to a similar extent.

We were confident of the reliable separation of urine and feces samples in the metabolic cages used. However, remaining radioactivity was encountered in the cage cone-collector walls and steel grid owing to urine dried on the way down to the collecting tubes. This partial radioactivity loss was reported in our previous study (*17*). This last observation did not prevent us from proceeding with analysis seeking the qualitative metabolic profile in the urine samples since remaining radioactivity was less than 2% of the administered dose in organ-tissues and feces. Thus, the urine samples accumulated the most substantial radioactivity clearance.

Analytical Determination and Identification of Metabolites in Urine Samples. Figure 1 shows the HPLC profiles of methanol-diluted urine aliquots obtained from β-NF-induced, (*S*)- and (*R*)-PAP-treated mice. Similarly to what was previously found in the experiments with *rac*-PAP (*17*), the ^{14}C-radioactivity traces (Figure 1, panels A and B) of both mouse strains treated with either enantiomer of PAP show a major peak at 16.2 min which, on average, accounts for approximately 62 ± 2% of the total integrated area. The second major peak in the radioactivity tracings of the C57BL/6 mice urine is found close to 4 min. It accounts for about 20% of the total integral, and it should contain the most polar PAP metabolites. Similar results were obtained for the A/J mice treated with (*S*)-PAP while those treated with (*R*)-PAP showed the same peak with a lower intensity. Other radioactive peaks were more clearly observed in this last tracing in the 5−10 and 16−20 min regions, which were less intense or absent in the other chromatograms.

The differential metabolism of (*S*)- and (*R*)-PAP becomes more evident in the UV-monitored chromatograms (Figure 1, panels C and D). The peak at 16.2 min (peak **g**) is again the major single peak on all traces. A minor peak with a retention time close to 20 min (peak **k**) is also present in the four chromatograms. These two peaks show the same UV spectrum (Figure 2) and can be assigned to 2-hydroxy-3-(phenylamino)propanoic acid (**1**) and PAP, respectively, based on the identity of their retention times and spectra with those of synthetic standards (*17*). The second major peak with a retention time close to 4 min (peak **a**) shows a nonhomogeneous UV spectrum (not shown) which suggests that it corresponds to the sum of several unresolved polar components in the urine samples, some of them being highly polar PAP metabolites. The spectra of peaks **b**−**e** and **h**−**i** are also shown in Figure 2, while those for peaks **f** and **j** are not included since they exhibit characteristics of overlapping signals, similar to peak **a**. Taking the spectrum of PAP (peak **k**) as reference, the spectra of peaks **b** and **d** show a bathochromic shift in the position of one of the maxima from 289 to 300 nm and a slight ipsochromic shift of the PAP maximum at 243 nm. Comparison of these spectra with those from synthetic standards **2**, **3b**, and **4a**,**b** (Chart 1) (*17*) suggests that **b** and **d** could correspond to phenolic PAP metabolites. On the other hand, the UV spectrum of peak **c** shows only a maximum at 243 nm and a shoulder close to 280 nm, which are similar to what is observed for standards that contain an acylated aniline moiety like acetanilide, paracetamol, or the *N*-acetyl derivative of PAP (*17*); these compounds, however, exhibited longer retention times under our chromatographic conditions. Peaks **e**, **h**, and **i** show PAP-like spectra with minor shifts in the position of their maxima, which suggests that these metabolites bear an intact aniline moiety and that the modifications should be located in the alkyl chain, as in acid **1**.

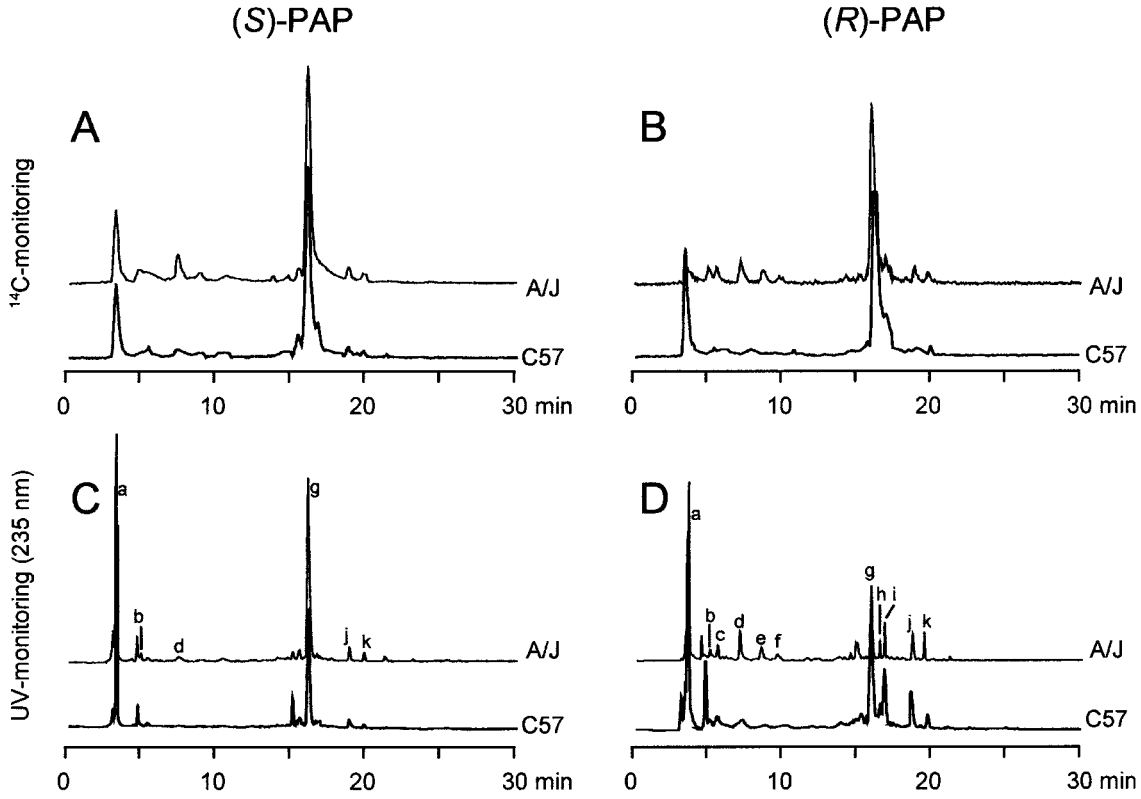

Figure 1. Typical HPLC chromatograms of methanol-diluted urine samples from *β*-NF-induced A/J and C57BL/6 mice treated with either (*S*)- or (*R*)-PAP spiked with [^{14}C]-*rac*-PAP. ^{14}C-radioactivity tracings are plotted 0.33 min to the left to correct for the dead volume between the on-line UV and radioactivity detectors. HPLC conditions are described under Materials and Methods.

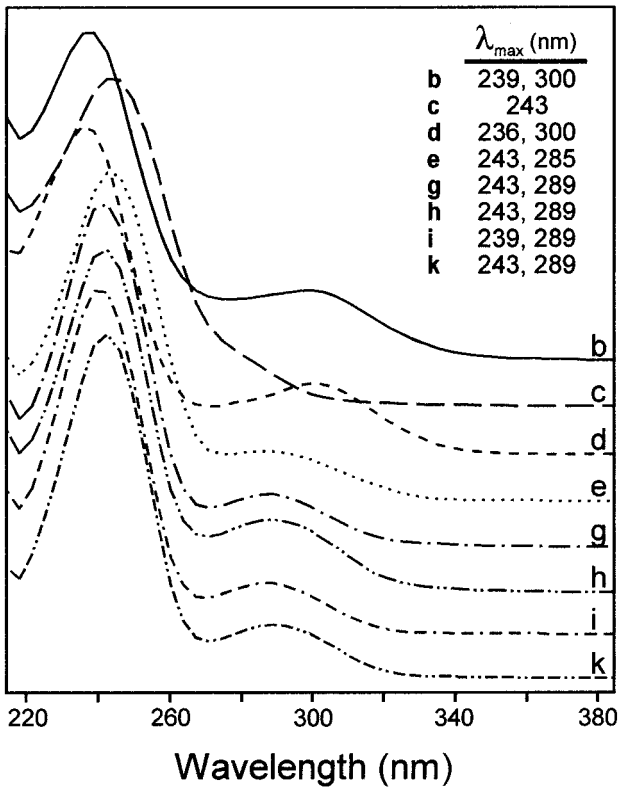

Figure 2. UV spectra extracted from the tracings shown in Figure 1 (panels C and D) for the peaks that show a corresponding signal in the radioactivity detector. Spectra of peaks **a**, **f**, and **j** are omitted since they show overlapping signals.

Although accurate quantitation of these metabolites in the different urine samples was beyond the scope of the present work, the chromatograms shown in panels C and D of Figure 1 provide information about the relative abundances of different metabolites. Thus, urine samples from mice treated with (*R*)-PAP contained a higher proportion (relative to the main single peak **g**) of metabolites that give rise to peaks **b**−**e** and **h**−**i** than those from mice treated with (*S*)-PAP. Mice treated with (*R*)-PAP show also a higher proportion, relative to **g**, of the peak assigned to PAP (**k**). The differences among peaks **a**, **f**, and **j** are less significant since, as stated above, their UV spectra indicate overlapping of two or more peaks. On the other hand, the profile differences observed between the A/J and the C57BL/6 mouse strains treated with either (*R*)- or (*S*)-PAP are less important.

The extraction of buffered urine samples with a mixture of dichloromethane−isopropyl alcohol−ammonia permitted the separation of PAP from most of its more polar metabolites. HPLC analysis of these organic extracts revealed, apart from PAP and minor amounts of acid **1** and other less abundant metabolites, a major radioactive peak (Figure 3, arrowed peak) which showed a counterpart in the DAD detector with maxima at 232 and 296 nm. The shape and relative abundance of this peak appeared to be dependent on sample history, but the peak could be detected in samples from both mouse strains treated with each PAP enantiomer. Analysis by GC/MS of the extracts treated with BSTFA permitted detection of a product with an EI-MS spectrum (Figure 3, bottom panel) consistent with the structure of the bis(trimethylsilyl) derivative of 4-aminophenol. Confirmation of the identity of this metabolite as 4-aminophenol was obtained from comparison of its chromatographic and spectroscopic data with those of an authentic standard.

In agreement with our previously reported study, the major metabolite in the urine samples identified as acid

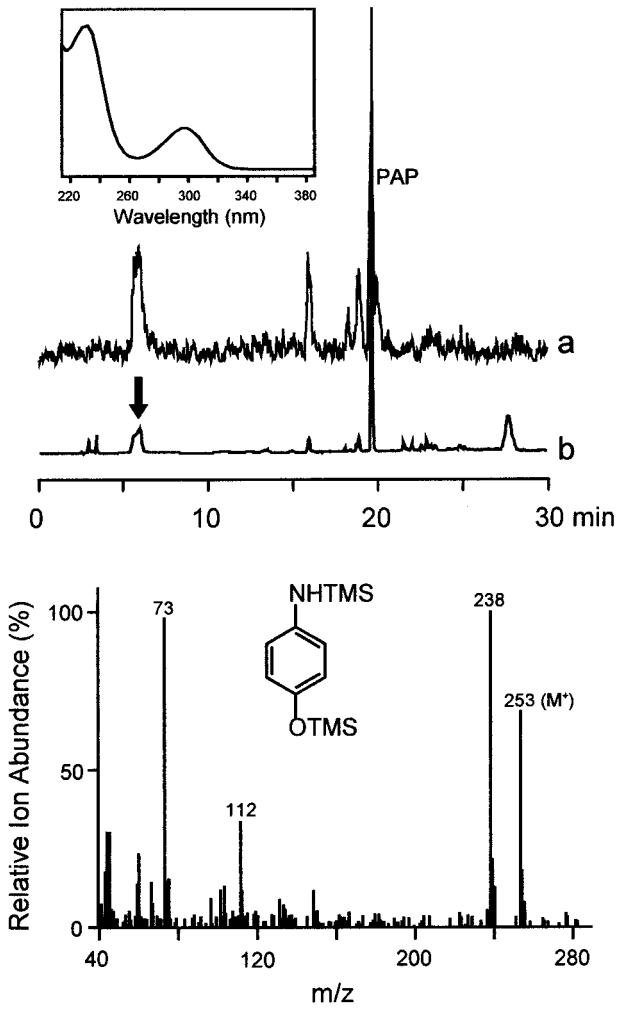

Figure 3. Typical HPLC chromatograms [upper panel, (a) ^{14}C-monitoring; (b) UV-monitoring] of organic extracts of buffered urine representative of both mouse strains treated with each PAP enantiomer [tracings correspond to (*R*)-PAP-treated A/J mice]. The PAP peak is labeled, and the UV spectrum of the peak labeled with an arrow is shown in the inset. Analysis by GC/MS, as described under Materials and Methods, permitted the detection of one product with an EI-MS spectrum (bottom panel) consistent with the bis(trimethylsilyl) derivative of 4-aminophenol.

1 (peak **g**, Figure 1), as well as the polar radioactive components appearing in the 3−4 min region and most of the other minor metabolites, remained in the aqueous phase. With the exception of the disappearance of acid **1** and the consequent formation of the corresponding methyl ester (*17*), treatment of lyophilized aliquots of these aqueous phases with HCl/MeOH caused only minor changes in the HPLC profiles.

Semipreparative HPLC injections of the urine samples and collection of individual peaks or groups of peaks were also carried out; these fractions were lyophilized, derivatized with BSTFA, and analyzed by GC/MS. As occurred in the experiments carried out with *rac*-PAP (*17*), the *O*-silylated derivative of acid **1** and the corresponding *O*-silylated derivatives of phenols **2** and **3a** could be detected in urine samples of mice treated with either of the two PAP enantiomers in the 3−10 min fraction. Moreover, a minor peak was detected in the 15−19 min fraction of urine samples from (*R*)-PAP-treated A/J mice, with an EI-MS spectrum showing a molecular ion at *m*/*z* 325 and a base peak at *m*/*z* 120. This product was already

Chart 2. PAP Derivative Structures Postulated from the Analysis by GC/MS of Urine Samples from PAP-Treated C57BL/6- and A/J-Strain Mice[a]

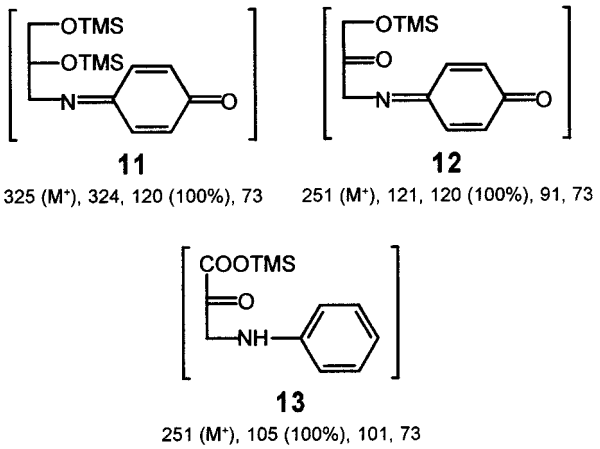

[a]The MS spectrum (*m*/*z*) main peak lists are given for each structure.

detected in the experiments with *rac*-PAP (*17*), and at that time, it was tentatively assigned to the quinoneimine derivative **11** (Chart 2). In the same collected fraction, two additional peaks were also detected which exhibited spectra with molecular ions at *m*/*z* 251 and base peaks at *m*/*z* 120 and 105, respectively, which are consistent with the ketonic structures **12** and **13** (Chart 2).

Further attempts for conjugate cleavage were carried out by treating urine samples with the glucuronidases from *E. coli* and *H. pomatia*, followed by organic extraction, as described under Materials and Methods. HPLC analysis of the aqueous phases showed the peak of acid **1**, at 16.2 min, as the main radioactive peak, while the polar radioactive components present in the untreated urine in the 3−10 min region (Figure 1) were absent or with considerably diminished intensity. In contrast, in addition to the peak of PAP, acid **1**, and 4-aminophenol already observed in the extracts of buffered urine (Figure 3), analysis of the organic phases showed a new peak with a retention time close to 14 min (Figure 4, arrowed peak) and a UV spectrum with a maximum at 243 nm and a shoulder at ∼280 nm, probably derived from the metabolite that gave rise to peak **c** in Figure 1. This peak was initially identified as paracetamol based on the comparison of its chromatographic mobility and UV spectrum with those of a commercial standard. Final confirmation of the structure of this metabolite was obtained by derivatization of these organic phases with BSTFA and analysis by GC/MS, which permitted the detection of a peak with a retention time and an EI-MS spectrum (Figure 4, bottom panel) identical to those exhibited by the bis(trimethylsilyl) derivative of paracetamol (*30*). These observations constitute strong evidence for the presence of paracetamol conjugates, which are well documented in the literature (*31*, *32*), in the urine samples of A/J and C57BL/6 mice treated with either of the two PAP enantiomers. The organic extracts after enzyme hydrolysis were enriched in a 15−20% radioactivity count compared with nonhydrolyzed extracted urine. This finding was consistent with the appearance of 4-aminophenol and paracetamol in the chromatographic profiles, and suggests glucuronide and sulfate conjugates for these metabolites. The possibility that these two metabolites could arise from the metabolism

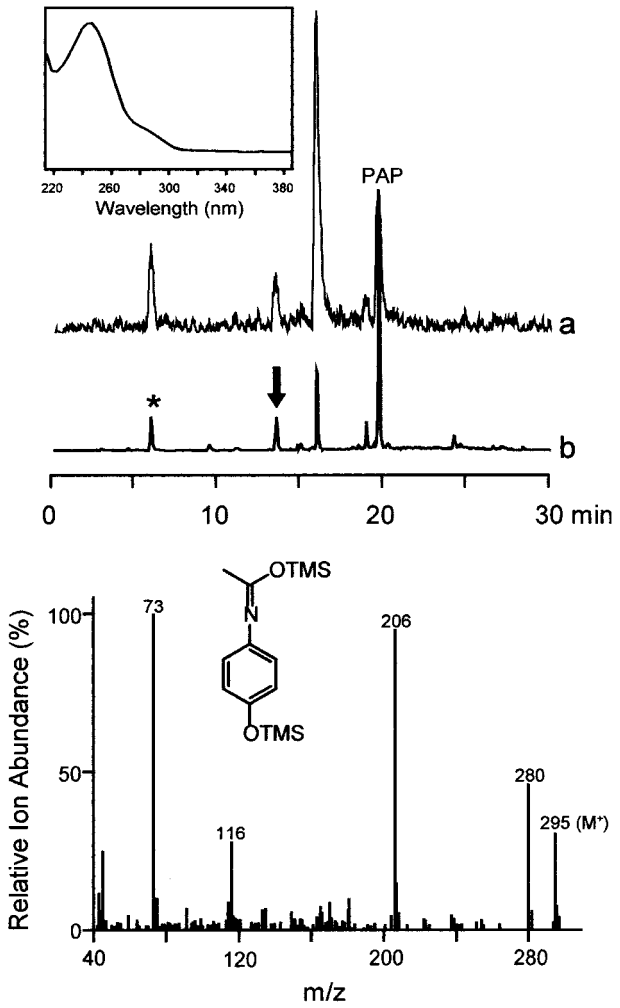

Figure 4. Typical HPLC chromatograms [upper panel, (a) ^{14}C-monitoring; (b) UV-monitoring] of organic extracts of *H. pomatia* β-glucuronidase hydrolysis representative of urine samples from both mice strains treated with each PAP enantiomer [tracings correspond to (*R*)-PAP-treated A/J mice]. The PAP peak is labeled as well as the peak of 4-aminophenol (asterisk). The UV spectrum of the peak labeled with an arrow is shown in the inset. Analysis by GC/MS, as described under Materials and Methods, permitted the detection of one product with an EI-MS spectrum (bottom panel) consistent with the bis(trimethylsilyl) derivative of paracetamol.

of residual aniline present in the PAP doses administered to mice was ruled out through careful analysis of PAP injection.

Discussion

Metabolism and clearance of intraperitoneally administered (*R*)- and (*S*)-PAP in A/J and C57BL/6 mice were studied, and several metabolites excreted in urine were identified. As previously reported for analogous experiments with *rac*-PAP (*17*), approximately 60% of the total radioactivity dose was found in urine samples of both mouse strains; thus, urine elimination is the main PAP clearance route. Analysis of urine samples from A/J and C57BL/6 strains revealed qualitatively similar compositions, with acid **1** as the major PAP derivative formed from both enantiomers; however, animals treated with (*R*)-PAP showed a higher proportion of other metabolites (Figure 1). Among these metabolites, phenolic derivatives of PAP (**2**) and the above-mentioned acid **1** (**3a**) were identified. These phenolic compounds are potential precursors of quinoneimine derivatives which could be formed through cytochrome P-450 or peroxidase-mediated oxidations, as described for the case of the known hepatotoxics paracetamol (*22*, *33*) and amodiaquine (*23*, *25*). In this respect, the detection of minor products which showed EI-MS spectral data consistent with the quinoneimine structures **11** and **12** is noteworthy.

The detection of such quinoneimine compounds in urine samples seems inconsistent with our current observations concerning the instability of the synthetic analogue **8**, which suggests that these products in aqueous medium could verify a rapid isomerization to the corresponding imines, followed by hydrolytic cleavage with ultimate release of 4-aminophenol. However, this possibility cannot be completely ruled out since the observation of a base peak at *m*/*z* 120 is consistent with fragmentation of the C2−C3 bond, which has been systematically observed for all PAP derivatives studied (*17*). In this respect, the detection of 4-aminophenol in the organic extracts of buffered urine samples constitutes additional indirect evidence of the presence of quinoneimine species in those urine samples. We also detected minor amounts of 4-aminophenol in samples of the purified standards **2**, **3b**, and **4a** (data not shown), which suggests that nonenzymatic formation of this product can be expected from molecules that contain such a 4-alkylaminophenol moiety.

Similar observations have been reported during the tyrosinase-catalyzed oxidation of *N*-(4-hydroxyphenyl)-glycine **4a** (*28*), as well as for the quinoneimine derivatives of 4-methylaminophenol and other alkylaminophenols (*29*). It has been described that the formation of 4-aminophenol occurs through prototropic rearrangement of the corresponding quinoneimines to give an imine which undergoes hydrolytic cleavage to yield 4-aminophenol and the corresponding aldehyde (Scheme 2). Our results indicate that such a mechanism can be extended to the PAP phenolic derivatives considered here.

Taken together, these observations suggest that different quinoneimine PAP derivatives could be generated in β-NF PAP-treated mouse strains. The possibility that these quinoneimine compounds are an artifact due to the spontaneous air oxidation of phenolic species such as **2** or **3a**, followed by a transformation pathway such as that indicated in Scheme 2, can be ruled out because of the detection of paracetamol in the same urine samples. The occurrence of paracetamol should be attributed to in vivo acetylation of 4-aminophenol (*34*); thus, it strongly indicates that these transformations must be part of the in vivo metabolic fate of PAP in mice.

The toxicological implications of these findings are important because they provide evidence, for the first time, that PAP metabolism can give rise to the formation of products, such as paracetamol and 4-aminophenol, with well-known toxicity. Furthermore, they suggest the formation of highly reactive quinoneimines which might be considered potentially toxic compounds, as well as other metabolites derived from further transformation of the alkyl chain, i.e., the α-keto acid precursor of the tentatively identified **13**. The range of PAP metabolites may be even wider if we consider the alkyl derivatives, probably aldehydes (Scheme 2), which should be released during the cleavage of the carbon−nitrogen bond that gives rise to the formation of 4-aminophenol. Additional structures are also plausible if we consider that similar transformations to those described in the oxidation of

N-(4-hydroxyphenyl)glycine (**4a**) (*28*), to give for instance muconic acid derivatives, may be taking place.

These findings have potential toxicological implications for TOS since patients could have had an enzyme activity impairment on pathways dealing with detoxification of PAP derivatives, resulting in the accumulation of reactive, unstable species similar to those reported here. In this respect, we recently reported that TOS survivors presented a specific profile derived from genetic polymorphisms on xenobiotic metabolism enzymes; in fact, impaired NAT-2 (acetylation) may have mediated susceptibility in those patients compared with their geographical controls (*16*). Moreover, reactive metabolites derived from xenobiotic metabolism have been associated with autoimmune diseases related to xenobiotic exposure (*35*, *36*), with immune activation being a crucial characteristic for TOS and EMS (*37*). In particular, aromatic oxidized species and quinoneimines have proved to induce some type of lymphocyte transformation (*35*, *36*, *38*).

To obtain an animal model in the future for in-depth study of TOS pathogenic mechanisms, the data of Berking et al. (*39*) add interest since they reported a Th2-lymphocyte pattern in the same mouse strains used in this study after OLA dosage given intraperitoneally. This Th2 pattern has also been reported in TOS patients (*40*). This interesting study indicated the possibility of reactive metabolites from oleanilides. In this respect, amidase hydrolysis of OLA can occur to yield aniline, and the aniline moiety possibly undergoes conjugation either by microsomal carboxylesterase enzymes (*41, 42*) or by acetylation (*34*). The latter acetanilide product can be metabolized to yield 4-aminophenol and paracetamol (*34*). Thus, a metabolic interaction between OLA and PAP derivatives could be postulated, and the metabolic findings (*16*) observed in TOS survivors (impaired acetylation) would have toxicological significance. Therefore, A/J and C57BL/6 mice could be considered good candidates for TOS-animal models, and our studies add a further step to determine the toxicokinetics necessary for future research seeking toxicity targets of these potentially toxic metabolites.

In relation to other clinically related diseases, a link between EMS and TOS has been suggested in the literature owing to the chemical similarities of PAA and PAP (*43, 44*). Even though we have not been able to detect PAA in urine in any of our experiments, our results suggest that PAA could suffer similar transformations to PAP to yield quinoneimine metabolites and generate 4-aminophenol and paracetamol. In this respect, phenolic metabolites from PAA-orally-administered rats had been reported (*19*). Confirmation of this point would establish an additional connection between the toxicokinetics of both compounds, which does not require necessarily their metabolic interconversion.

In summary, the results presented here indicate that (*R*)- and (*S*)-PAP are metabolized in A/J and C57BL/6 β-NF-induced mice to yield a wide range of polar derivatives, with higher rates observed for the (*R*)-PAP enantiomer. Some of these polar metabolites are easily cleared from the organism in urine, i.e., acid **1**, and may constitute a major detoxifying route in those mice, whereas some others are highly reactive compounds. The observation that samples of some of the phenolic compounds considered here (**2**, **3b**, and **4a**) spontaneously generate 4-aminophenol, presumably through the formation of a quinoneimine intermediate, suggests the possible generation of some of these species in a nonenzymatic way in different tissues, and their possible reaction with macromolecules in a widespread manner after higher, or accumulation of, PAP doses.

Acknowledgment. This work was supported by Grant FIS-97/1317-SAT of the Fondo de Investigación Sanitaria of the Spanish Ministry of Health. Ms. C. O'Hara kindly revised the English version of the manuscript.

References

(1) Gradjean, P., and Tarkowski, S., Eds. (1984) *Toxic Oil Syndrome: mass food poisoning in Spain. Report of a WHO Meeting: Madrid, 21−25 March, 1983*, World Health Organisation Regional Office for Europe, Copenhagen, Denmark.

(2) Tabuenca, J. M. (1981) Toxic allergic syndrome caused by ingestion of rapeseed oil denatured with aniline. *Lancet* **2**, 567−568.

(3) Diaz de Rojas, F., Castro-García, M., Abaitua-Borda, I., Alonso-Gordo, J. M., Posada de la Paz, M., Kilbourne, E. M., and Tabuenca-Oliver, J. M. (1987) The association of oil ingestion with Toxic Oil Syndrome in two convents. *Am. J. Epidemiol.* **125**, 907−911.

(4) Cañas, R., and Kilbourne, E. M. (1987) Oil ingestion and the Toxic Oil Syndrome. Results of a survey of residents of the Orcasur neighborhood in Madrid Spain. *Int. J. Epidemiol.* **16**, 3−6.

(5) Rigau-Perez, J. G. (1984) Summary of case-control studies and case or cluster investigations. In *Toxic Oil Syndrome: mass food poisoning in Spain. Report of a WHO Meeting: Madrid, 21−25 March, 1983* (Gradjean, P., and Tarkowski, S., Eds.) pp 47−51, World Health Organisation Regional Office for Europe, Copenhagen, Denmark.

(6) Rigau-Perez, J. G., Pérez-Alvarez, L., Dueñas-Castro, S., Choi, K., Thacker, S. B., Germain, J. L., González-de-Andrés, G., Canada-Royo, L., and Pérez-Gallardo, F. (1984) Epidemiologic investigation of an oil-associated pneumonic paralytic eosinophilic syndrome in Spain. *Am. J. Epidemiol.* **119**, 250−260.

(7) Bernert, J. T., Kilbourne, E. M., Akins, J. R., Posada de la Paz, M., Meredith, N. K., Abaitua-Borda, I., and Wages, S. (1987) Compositional analysis of oil samples implicated in the Spanish toxic oil syndrome. *J. Food Sci.* **52**, 1562−1569.

(8) Vázquez-Roncero, A., Janer del Valle, C., Maestro-Duran, R., and Graciane-Constante, E. (1983) New aniline derivatives in cooking oils associated with the toxic oil syndrome. *Lancet* **2**, 1024−1025.

(9) Hill, R. H., Schurz, H. H., Posada de la Paz, M., Abaitua-Borda, I., Philen, R. M., Kilbourne, E. M., Head, S. L., Bailey, S. L., Driskell, W. J., Barr, J. R., and Needham, L. L. (1995) Possible etiologic agents for Toxic Oil Syndrome: fatty acid esters of 3-(*N*-phenylamino)-1,2-propanediol. *Arch. Environ. Contam. Toxicol.* **28**, 259−264.

(10) Posada de la Paz, M., Philen, R. M., Schurz, H. H., Hill, R. H., Gimenez-Ribota, O., Gómez de la Cámara, A., Kilbourne, E. M., and Abaitua-Borda, I. (1999) Epidemiologic evidence for a new class of compounds associated with Toxic Oil Syndrome. *Epidemiology* **10**, 130−134.

(11) Posada de la Paz, M., Philen, R. M., Abaitua Borda, I., Bernert, J. T., Bada-Gancedo, J. C., DuClos, P. J., and Kilbourne, E. M. (1996) Toxic Oil Syndrome: traceback of the toxic oil and evidence for a point source epidemic. *Food Chem. Toxicol.* **34**, 251−257.

(12) Aldridge, W. N. (1992) Experimental studies. In *Toxic Oil Syndrome: current knowledge and future perspectives* (Nadal, J., and Tarkowski, S., Eds.) pp 63−93, WHO Regional Publications: European Series 42, World Health Organization Regional Office for Europe, Copenhagen, Denmark.

(13) Vázquez-Roncero, A., Maestro-Duran, R., and Ruiz-Gutierrez, V. (1984) New aniline derivatives in oils related to the Toxic Syndrome. Toxicity in mice of 3-phenylamino-1,2-propanediol and its fatty acid mono- and diesters. *Grasas Aceites (Sevilla)* **35**, 330−331.

(14) Maestro-Duran, R., Ruiz-Gutierrez, V., and Vázquez-Roncero, A. (1986) Toxic Oil Syndrome in Spain: toxicological study in mice of new aniline derivatives present in toxic oils. *Grasas Aceites (Sevilla)* **37** (4), 207−214.

(15) Ruiz-Gutierrez, V., and Maestro-Duran, R. (1992) Lymphatic absorption of 3-phenyalmino-1,2-propanediol and its esters. *Exp. Toxicol. Pathol.* **44**, 29−33.

(16) Ladona, M. G., Izquierdo, M., Posada de la Paz, M., De la Torre, R., Ampurdanés, C., Segura, J., and Sanz, E. (2001) Pharmacogenetic profile of xenobiotic enzyme metabolism in survivors of the Spanish Toxic Oil Syndrome. *Environ. Health Perspect.* **109**, 369−375.

(17) Ladona, M. G., Bujons, J., Messeguer, A., Ampurdanés, C., Morató, A., and Corbella, J. (1999) Biotransformation and clearance of 3-(phenylamino)propane-1,2-diol, a compound present in samples related to Toxic Oil Syndrome, in C57BL/6 and A/J mice. *Chem. Res. Toxicol.* **12**, 1127−1137.

(18) Dahlin, D. C., and Nelson, S. D. (1982) Synthesis, decomposition kinetics, and preliminary toxicological studies of pure *N*-acetyl-*p*-benzoquinone imine, a proposed toxic metabolite of acetaminophen. *J. Med. Chem.* **25**, 885−886.

(19) Adachi, J., Mio, T., Ueno, Y., Naito, T., Nishimura, A., Fujiwara, S., Sumino, K., and Tatsuno, Y. (1994) Identification of four metabolites of 3-(phenylamino)alanine, a constituent in L-tryptophan products implicated in eosinophilia−myalgia syndrome, in rats. *Arch. Toxicol.* **68**, 500−505.

(20) Islam, I., Skibo, E. B., Dorr, R. T., and Alberts, D. S. (1991) Structure−activity studies of antitumour agents based on pyrrolo-[1,2-a]benzimidazoles: New reductive alkylating DNA cleaving agents. *J. Med. Chem.* **34**, 2954−2961.

(21) Zimmer, H., Lankin, D. C., and Horgan, S. W. (1970) Oxidations with potassium nitrosodisulfonate (Fremy's radical). The Teuber reaction. *Chem. Rev.* **71**, 229−246.

(22) Potter, D. W., and Hinson, J. A. (1987) Mechanisms of paracetamol oxidation to *N*-acetyl-*p*-benzoquinone imine by horseradish peroxidase and cytochrome P-450. *J. Biol. Chem.* **262**, 966−973.

(23) Thompson, C. D., Vachaspati, P. R., Kolis, S. P., Gulden, P. H., Garst, M. E., Wiese, A., Munk, S. A., Harman, W. D., and Macdonald, T. L. (1997) A proposed mechanism for *p*-aminoclonidine allergenicity based on its relative oxidative lability. *Chem. Res. Toxicol.* **10**, 1032−1036.

(24) Bolton, J. L., Trush, M. A., Penning, T. M., Dryhurst, G., and Monks, T. J. (2000) Role of quinones in toxicology. *Chem. Res. Toxicol.* **13**, 135−160.

(25) Harrison, A. C., Kitteringham, N. R., Clarke, J. B., and Park, B. K. (1992) The mechanism of bioactivation and antigen formation of amodiaquine in the rat. *Biochem. Pharmacol.* **43**, 1421−1430.

(26) Bessems, J. G. M., Te Koppele, J. M., van Dijk, P. A., van Stee, L. L. P., Commandeur, J. N. M., and Vermeulen, N. P. E. (1996) Rat liver microsomal cytochrome P450-dependent oxidation of 3,5-disubstituted analogues of paracetamol. *Xenobiotica* **26**, 647−666.

(27) Zeller, K. P., and Müller, R. (1988) Mass spectra of quinones. In *The Chemistry of functional groups. The Chemistry of quinonoid compounds* (Patai, S., and Rappoport, Z., Eds.) Vol. 2, pp 1231−1292, J. Wiley & Sons, Chichester, U.K.

(28) Mascagna, D., Costantini, C., d'Ischia, M., and Prota, G. (1992) Tyrosinase-catalyzed oxidation of the new melanocytotoxic agent *N*-4-hydroxyphenylglycine: unusual cleavage of the 4-aminophenol ring to muconic semialdehyde derivatives. *Tetrahedron* **48**, 8309−8316.

(29) Brown, E. R. (1988) Quinonediimines, monoimines and related compounds. In *The Chemistry of functional groups. The Chemistry of quinonoid compounds* (Patai, S., and Rappoport, Z., Eds.) Vol. 2, pp 1231−1292, J. Wiley & Sons, Chichester, U.K.

(30) Baty, J. D., Robinson, P. R., and Wharton, J. (1976) A method for the estimation of acetanilide, paracetamol and phenacetin in plasma and urine using mass fragmentography. *Biomed. Mass Spectrom.* **3**, 60−63.

(31) Andrews, R. S., Bond, C. C., Burnett, J., Saunders, A., and Watson, K. (1976) Isolation and identification of paracetamol metabolites. *J. Int. Med. Res.* **4**, 34−39.

(32) Watari, N., Iwai, M., and Kaneniwa, N. (1983) Pharmacokinetic study of the fate of paracetamol and its conjugates in rats. *J. Pharmacokinet. Biopharm.* **11**, 245−272.

(33) Potter, D. W., and Hinson, J. A. (1987) The 1- and 2-electron oxidation of paracetamol catalyzed by prostaglandin H synthase. *J. Biol. Chem.* **262**, 974−980.

(34) Gorrod, J. W., and Manson, D. (1986) The metabolism of aromatic amines. *Xenobiotica* **16**, 933−955.

(35) Griem, P., Wulferink, M., Sachs, B., Gónzalez, J. B., and Gleichmann, E. (1998) Allergic and autoimmune reactions due to xenobiotics: how do they arise? *Immunol. Today* **19**, 133−141.

(36) Hess, D. A., and Rieder, M. J. (1997) The role of reactive drug metabolites in immune-mediated adverse drug reactions. *Ann. Pharmacother.* **31**, 1378−1387.

(37) Philen, R. M., and Posada de la Paz, M. (1993) Toxic Oil Syndrome and Eosinophilia Myalgia Syndrome: May 8−10, 1991, World Health Organization Meeting Report. *Semin. Arthritis Rheum.* **23**, 104−124.

(38) Kubicka-Muranyi, M., Goebels, R., Goebel, C., Uetrecht, J., and Gleichmann, E. (1993) T Lymphocytes ignore procainamide, but respond to its reactive metabolites in peritoneal cells: demonstration by the adoptive transfer popliteal lymph node assay. *Toxicol. Appl. Pharmacol.* **122**, 88−94.

(39) Berking, C., Hobbs, M. V., Chatelain, R., Meurer, M., and Bell, S. A. (1998) Strain-dependent cytokine profile and susceptibility to oleic acid anilide in a murine model of the Toxic Oil Syndrome. *Toxicol. Appl. Pharmacol.* **148**, 222−228.

(40) del Pozo, V., de Andrés, B., Gallardo, S., Cardaba, B., de Arruda-Chaves, E., Cortegano, I., Jurado, A., Palomino, P., Oliva, H., Aguilera, B., Posada, M., and Lahoz, C. (1997) Cytokine mRNA expression in lung tissue from Toxic Oil Syndrome patients: a Th2 immunological mechanism. *Toxicology* **118**, 61−70.

(41) Kaphalia, B. S., Fritz, R. R., and Ansari, G. A. S. (1977) Purification and characterization of rat liver microsomal fatty acid ethyl and 2-chloroethyl ester synthase and their relationship with carboxylesterase (p*I* 6.1). *Chem. Res. Toxicol.* **11**, 211−218.

(42) Kaphalia, B. S., Green, S. M., and Ansari, G. A. S. (1999) Fatty acid ethyl and methyl ester synthases, and fatty acid anilide synthase in HepG2 and AR42J cells: interrelationships and inhibition by tri-*o*-tolyl phosphate. *Toxicol. Appl. Pharmacol.* **159**, 134−141.

(43) Mayeno, A. N., Belongia, E. A., Lin, F., Lundy, S. K., and Gleich, G. J. (1992) 3-(Phenylamino)alanine, a novel aniline-derived amino acid associated with the eosinophilia−myalgia syndrome: a link to the toxic oil syndrome? *Mayo Clin. Proc.* **67**, 1134−1139.

(44) Mayeno, A. N., Benson, L. M., Naylor, S., Colberg-Beers, M., Puchalski, J. T., and Gleich, G. J. (1995) Biotransformation of 3-(phenylamino)-1,2-propanediol to 3-(phenylamino)alanine: a chemical link between Toxic Oil Syndrome and Eosinophilia−Myalgia Syndrome. *Chem. Res. Toxicol.* **8**, 911−916.

TX010001K